Molecular Cell, Vol. 12, 577–589, September, 2003, Copyright ©2003 by Cell Press

Convergent Mechanisms for Recognition of Divergent Cytokines by the Shared Signaling Receptor gp130

Martin J. Boulanger,[1] Alexander J. Bankovich,[1] Tanja Kortemme,[2] David Baker,[2] and K. Christopher Garcia[1,*]
[1]Department of Microbiology and Immunology
Department of Structural Biology
Stanford University School of Medicine
Fairchild D319, 299 Campus Drive
Stanford, California 94305
[2]Howard Hughes Medical Institute and
Department of Biochemistry
University of Washington
Seattle, Washington 98195

Summary

Gp130 is a shared cell-surface signaling receptor for at least ten different hematopoietic cytokines, but the basis of its degenerate recognition properties is unknown. We have determined the crystal structure of human leukemia inhibitory factor (LIF) bound to the cytokine binding region (CHR) of gp130 at 2.5 Å resolution. Strikingly, we find that the shared binding site on gp130 has an entirely rigid core, while the LIF binding interface diverges sharply in structure and chemistry from that of other gp130 ligands. Dissection of the LIF-gp130 interface, along with comparative studies of other gp130 cytokines, reveal that gp130 has evolved a "thermodynamic plasticity" that is relatively insensitive to ligand structure, to enable crossreactivity. These observations reveal a novel and alternative mechanism for degenerate recognition from that of structural plasticity.

Introduction

One of the hallmarks of four-helix bundle cytokines (e.g., interleukins, interferons, growth hormones, etc.) is their inducement of remarkably pleiotropic functional outcomes, in a variety of cell types. This pleiotropy is derived from the fact that multiple cytokine activities are funneled through a limited set of "shared" cell-surface signaling receptors such as gp130 and leukemia inhibitory factor receptor (LIF-R). These shared receptors mediate the functional outcomes of cytokine receptor engagement through overlapping, and often redundant, intracellular phosphorylation cascades largely involving Jak and STAT family members (Heinrich et al., 1998; Taga and Kishimoto, 1997). However, each cytokine also has its own unique spectrum of activities, which is achieved through the assembly of precisely organized extracellular receptor/ligand complexes, whose proximity and orientational differences can lead to qualitatively different signaling outcomes (e.g., EPO) (Livnah et al., 1996).

Gp130 is a remarkably crossreactive shared signaling receptor that is activated by ten, or more, four-helix cytokines that have been variously termed "gp130-cytokines" or "IL-6-type cytokines" (Hirano et al., 1997; Simpson et al., 1997). Some gp130-cytokines, such as Interleukin-6 (IL-6), Interleukin-11 (IL-11), and viral IL-6 utilize only gp130, in combination with their respective α-receptors, for signaling. Others, such as leukemia inhibitory factor (LIF), oncostatin (OSM), cardiotrophin (CT-1), and ciliary neurotrophic factor (CNTF) incorporate gp130 into a heterocomplex with LIF receptor, which is a second shared receptor for gp130-cytokines (Figure 1A) (Benigni et al., 1996; Hibi et al., 1990; Taga and Kishimoto, 1997). Gp130 and LIF-R have domain architectures of six and eight contiguous β sandwich domains, containing one or two signature cytokine binding regions (CHR) (Bazan, 1990), respectively, and a single Ig-domain (IgD), which is dispensable for LIF binding and activation (Hammacher et al., 1998).

Leukemia inhibitory factor (LIF) is a highly pleiotropic member of the long-chain family of four-helix bundle cytokines (Hilton et al., 1988), whose activities include suppression of leukemic cell growth, maintenance of pluripotentiality of murine embroynic stem cells, potent regulation of inflammatory responses (Gyotoku et al., 2001), induction of growth in neuronal tissues (Murphy et al., 1991; Yamamori et al., 1989), and inhibition of placental HIV replication (Patterson et al., 2001). Clearly the diverse range of LIF activities on a variety of cell types suggests a strong potential for therapeutic applications if the specificity determinants can be delineated, and subsequently utilized, to minimize the functional pleiotropy. This problem has limited the utility of the gp130 system, as well as other shared receptor systems, as therapeutic entry points.

While gp130 engagement of LIF is thought to be mediated by a LIF "site II" (Figure 1A), the higher-order signaling assembly containing LIF-R has been attributed to an additional receptor binding epitope, termed "site III" (Figure 1A) that is unique to the gp130-class cytokines. No structural information exists regarding complex formation between LIF and gp130 or LIF-R, and the assembly mechanism of the higher order complex has not been determined.

Our principal aims in this study are to (1) determine the molecular basis by which gp130 serves as a shared receptor for structurally dissimilar cytokine surfaces, and (2) delineate the composition and assembly pathway of the LIF/gp130/LIF-R extracellular signaling complex. Toward this end, we have elucidated the structure of the complex between LIF and gp130 (Figures 2A–2D; Table 1) and defined the binding determinants that are both shared and unique to this receptor/ligand pair (Figures 3A–3C). Contrary to the accepted paradigm of conformational change within cytokine receptor binding sites as an adaptation mechanism, gp130 is rigid, lacking even side chain rotamer movement in the interface upon binding. Computational energetic mapping of the viral-IL-6 and LIF-gp130 interfaces reveals opposing energetic landscapes for each cytokine mediated by identical residues on the receptor, but different residues on the cytokines (Table 2). We have measured the thermo-

*Correspondence: kcgarcia@stanford.edu

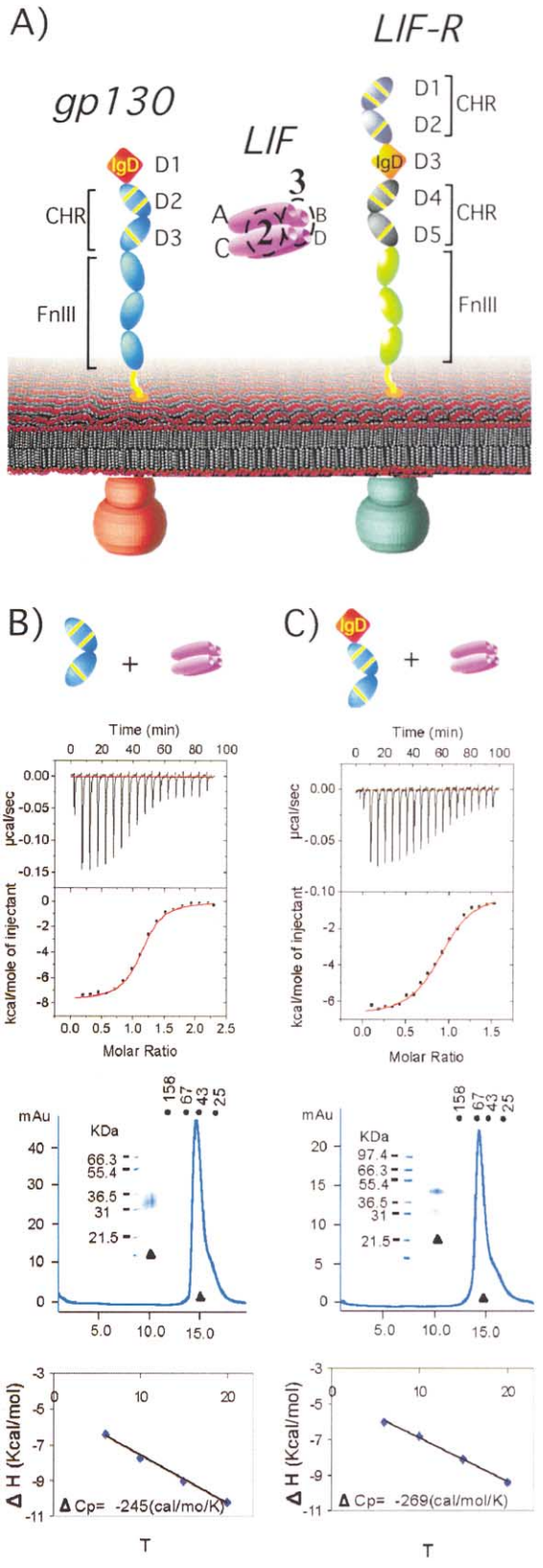

Figure 1. The LIF Cytokine Interactions

(A) Schematized view of the domain structure of gp130, LIF, and LIF-receptor (LIF-R). The immunoglobulin domain is represented by the D1 domain in gp130 (red) and the D3 domain in LIF-R (orange). CHR denotes the "cytokine binding homology region" and FnIII refers to the "fibronectin type-III domains." Yellow lines represent conserved disulfide bonds in the D2 domains and a conserved WSXWS motif in the D3 domain of the CHRs. Isothermal titration calorimtey of LIF with (B) gp130 D2D3 and (C) gp130 D1D2D3 showing that the D1 domain of gp130 does not affect bimolecular complex formation with LIF. The binding affinity Kd = 170 nM, stoichiometry (n) 0.94, enthalpy (ΔH) –6.99 Kcal/mol, entropy (ΔS) 6.07 (cal/molK) and heat capacity (ΔCp) –269 (cal/molK) measured for LIF-gp130D1D2D3 are similar to those measured for LIF-gp130-D2D3 (see Figure 4E). Following each titration, the protein complexes were run on a sizing column and visualized on an SDS-PAGE gel. Both of the bimolecular titrations were measured at four different temperatures (6, 10, 15, and 20 C°) and the heat capacity measured from the slope of the change in enthalpy plotted against temperature (bottom panel).

dynamics of the individual site II interactions for LIF, human IL-6, OSM, and CNTF, and find that, despite the ligand structural differences that give rise to unique interface chemistries, water expulsion appears to be the structurally insensitive, convergent entropic mechanism by which gp130 is endowed with such startling cross-reactivity (Figure 4). This mechanism contrasts sharply with the more accepted mechanisms of structural plasticity, which are expected to be limited by a narrow range of ligand structure, and an entropic penalty for conformational change.

Results and Discussion

LIF Binds Independently to the CHR Domains of gp130

We first dissected the LIF/gp130/LIF-R ectodomain-signaling complex into its component bi- and trimolecular interactions (schematized in Figure 1A). Can LIF independently bind to gp130 and LIF-R, or is there a cooperative interdependence to form the trimolecular signaling complex as seen for the human IL-6 hexamer (Boulanger et al., 2003)? We expressed a series of soluble, modular constructs of these receptors, and find that domains D1-D3 or D2D3 (e.g., the "CHR") of gp130 display the same binding thermodynamics in forming bimolecular complexes with LIF (Figures 1B and 1C) consistent with previous studies where the D1 domain of gp130 was shown to be dispensable for signaling by LIF (Hammacher et al., 1998). LIF-R D1-D5 was used in titrations with LIF (Figure 6A) to form a bimolecular complex while studies with the truncated constructs, D1-D3 and D3-D5 of LIFR, were unsuccessful due to low solubility of the receptor fragments (data not shown). We crystallized the complex of LIF with the gp130 CHR, which contains the receptor's shared binding site, and determined the structure to a resolution of 2.5 Å.

Structure of the LIF/gp130 Complex

In the complex, the D2 and D3 domains of gp130, which form the cytokine binding homology regions (CHR), form an elbow-shaped module, bent at an angle of ~90°, that interacts with the A and C helical faces of LIF to form the site II interface (Figure 2A). The overall structure of the gp130-CHR is essentially identical to that of the previously determined liganded structure of gp130 with both human (Boulanger et al., 2003) and viral Interleukin-6

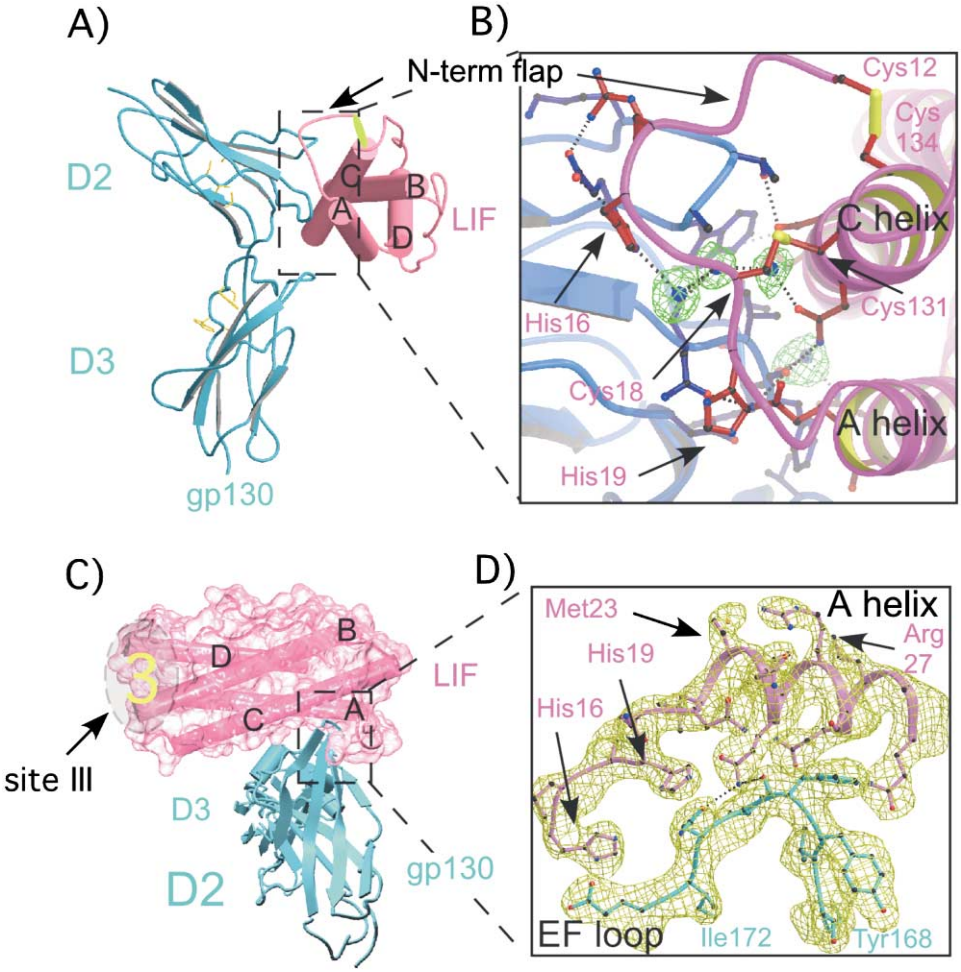

Figure 2. Structural Topology of the LIF/gp130 D2D3 Crystal Structure

(A) Backbone structure as viewed from the side of the LIF/gp130 complex.

(B) Close-up view of the interface showing four clear spheres of electron density (green) calculated at 2.5 σ from an omit map representing buried solvent molecules.

(C) "Top" view of the LIF/gp130 complex showing LIF bound to gp130 through its N-terminal region and the N-terminal flap.

(D) Close-up view of omit map electron density contoured at 2.5 σ showing the well-ordered N-terminal flap. Molscript (Kraulis, 1991) and Raster3D (Merritt and Murphy, 1994) were used to prepare secondary structure figures and Bobscript (Esnouf, 1997) was used to prepare electron density figures.

(r.m.s.d. of 0.8 Å for the α carbons) (Chow et al., 2001) and to an unliganded gp130 structure (r.m.s.d. of less than 1.5 Å for all α carbons of CHR domain) (Bravo et al., 1998). Strikingly, all but two of the 24 solvent-exposed side-chains that define the molecular contact surface adopt the *same* rotameric conformations in all three structures (Figure 3C). While the D2D3 inter-domain rigidity is not, in itself, noteworthy, the absence of torsional flexibility in 22 of the 24 contacting side chain dihedral angles within a solvent exposed, promiscuous binding site is surprising. Hence, the gp130 binding surface appears to be of unusual rigidity for a crossreactive binding surface, which are often endowed with structural plasticity to adapt to different ligands (Atwell et al., 1997). For example, structural plasticity is the mechanism used for recognition of hGH variants by the hGH receptor (Atwell et al., 1997), and T cell receptors have been shown to undergo dramatic conformational changes in the binding site to accommodate different peptide-MHC ligand structures (Garcia et al., 1998).

The structure of human LIF is a four-helix bundle upon which a unique N-terminal "flap" preceding helix A is tethered at both ends by disulfide bonds (Cys12-Cys134 and Cys18-Cys131) and forms a protruding lip at the base of the four-helix bundle (Figure 2B). LIF interacts primarily with the D2 domain of gp130 (Figure 2A), rather than within the "elbow" formed by the D2D3 bend, which was the binding strategy observed both in the viral IL-6/gp130 (D1D2D3) structure (Chow et al., 2001) and the human IL-6 hexameric complex structure (Boulanger et al., 2003). LIF helices A and C, and the N-terminal flap that precedes helix A, contribute the site II contact residues with gp130. The gp130 binding epitope of LIF (also called site II) is positioned toward the extreme N-terminal end of the four-helix bundle (Figures 2A and 2B). Since LIF does not possess an α-receptor analogous to

Table 1. Data Collection and Refinement Statistics

Crystallographic Statistics	
Data Collection	
Spacegroup	$P2_12_12_1$
Unit cell (Å) (a, b, c)	79.91 87.05 147.63
Source	ALS–BL 8.2.1
Resolution (Å) (highest resolution shell)	50–2.5 (2.63–2.5)
Measured reflections	463,823
Unique reflections	35,908
Completeness (%)	91.0 (78.4)
$I/\sigma(I)$	10.4 (1.5)
R_{merge}[a]	0.085 (0.511)
Refinement Statistics	
Resolution range (Å)	40 – 2.5
R_{cryst}[b]	0.248 (0.374)
R_{free}[c]	0.288 (0.415)
Number of atoms (protein, solvent)	5,796 192
R.m.s. deviation from ideality	
Bond lengths (Å)	0.010
Bond angles (°)	1.5
Dihedral angles (°)	22.9
Improper angles (°)	0.94

[a] $R_{merge} = \Sigma_{hkl}|I - <I>|/\Sigma_{hkl}I$, where I is the intensity of unique reflection hkl, and $<I>$ is the average over symmetry-related observation of unique reflection hkl.
[b] $R_{cryst} = \Sigma||F_{fobs} - F_{calc}|/\Sigma F_{fobs}$, where F_{obs} and F_{calc} are the observed and the calculated structure factors, respectively.
[c] R_{free} is calculated using 5% of reflections sequestered before refinement.

human IL-6 Rα, it does not have a functional site I, which is located on the face of cytokine B and D helices (Boulanger et al., 2003). However, the presumed site III (tip of four-helix bundle) of LIF is clearly accessible, presumably for binding to LIF-R in the higher order complex (discussed below).

The N-Terminal Flap of LIF as a "Molecular Doorstop"

The extended N-terminal loop of LIF, which is also observed in the unliganded structure of murine LIF (Robinson et al., 1994), is unique among the gp130 family of cytokines and the structure in complex with gp130 provides a functional rationale for this unusual structural feature. The flap effectively buttresses gp130 on one side, rigidifying the complex. The flap also creates an obvious shape complementarity in the interface through formation of a concave pocket that packs snugly against the convex CD loop of gp130CHR. In the complex, the N-terminal loop of LIF accounts for nearly 45% of the buried surface area contributed by LIF and is well ordered (Figure 2D), due to multiple interatomic stabilizing interactions. When comparing the structures of the liganded and unliganded human LIF (r.m.s.d. of 1.2 Å for α carbons) this polypeptide segment is displaced by gp130 CD loop away from the main body of the cytokine.

LIF Utilizes Polar Interactions to Contact gp130

The interface (~1400 Å^2 total buried surface area) between LIF and gp130 is largely hydrophilic, as evidenced by four well-defined solvent atoms that participate in an intermolecular hydrogen bond network bridging LIF with gp130 (Figure 2B). The majority of the polar residues are contributed by LIF. Gp130, on the other hand, contributes an approximately equal mix of polar and apolar residues to the binding interface (Figure 3D), highlighting an amphipathic capability likely necessary for the chemically diverse ligand surfaces with which it interacts (discussed below). A total of 20 residues from the A and C helices, which lie in two parallel grooves on the surface of gp130 and the N-terminal loop form the contact surface of LIF (~700 Å^2 buried surface area). The CD and EF interstrand loops of the D2 domain and the BC loop of the D3 domain form the binding surface of gp130 contributing a total of 19 residues and a similar buried surface area of 710 Å^2. In total, the binding interface is stabilized through nine protein-protein hydrogen bonds, eight solvent hydrogen bonds, and one salt bridge (Figure 2B).

Divergent Cytokine Binding Surfaces, Convergent gp130 Binding Site

A structural comparison of the LIF/gp130 complex with the previously determined vIL-6/gp130 (Chow et al., 2001) and human IL-6/Rα/gp130 complexes (Boulanger et al., 2003) reveal that, although the cytokine binding surfaces are highly divergent in position and chemistry, a core shared region on gp130 dominates ligand binding (Figures 3A and 3B). Due to the lower resolution of 3.65 Å of the human IL-6 hexamer structure (Boulanger et al., 2003), we restrict our discussion of detailed interatomic interactions to a comparison of the LIF/gp130 (2.5 Å) and viral IL-6/gp130 (2.4 Å) (Chow et al., 2001) complexes. Gp130 residues that *uniquely* interact with LIF or vIL-6 decorate the periphery of the core (Figures 3A–3C). Importantly, these specificity determinants indicate the possibility of designing cytokine-specific antagonists, rather than broadly neutralizing inhibitors, which has severely hampered the utility of shared receptors as drug targets. The thirteen shared residues of gp130 in the core contribute 66% and 88% to the total buried surface area to the LIF and vIL-6 complexes, respectively, indicating that viral IL-6 relies more heavily on the "shared core" of gp130. Despite the centralized docking surface of gp130, the overall viral IL-6 docking site on gp130 is shifted downward toward the D3 domain of gp130 where Ser^{229} and Val^{230} contribute 16.5% of the buried surface area relative to LIF where these residues contribute only 3.5% of the buried surface area. Again, these differences denote "specificity islands" that provide obvious target regions for cytokine-specific pharmaceuticals.

The shared regions of gp130 within the interfaces are utilized in chemically distinct fashions, with the cytokine-receptor contacts composed primarily of polar and apolar residues for LIF and vIL-6, respectively (Figure 3D). Gp130, then, appears capable of manufacturing high affinity for cytokines through either polar or apolar interactions from the same binding site, in the absence of conformational change. Many of the interface residues on gp130 that are involved strictly in van der Waals contacts with vIL-6 now participate in polar interactions with LIF. Asn^{171} and Asp^{193} of gp130 now participate in hydrogen bonds with Asn^{25} of LIF. This effect is also observed with Thr^{144} that forms a hydrogen bond with Ser^{127} of LIF. Ser^{165} on gp130 shifts slightly to facilitate hydrogen bond formation with Asp^{120} of LIF. In the case of viral IL-6, the almost exclusively hydrophobic contact

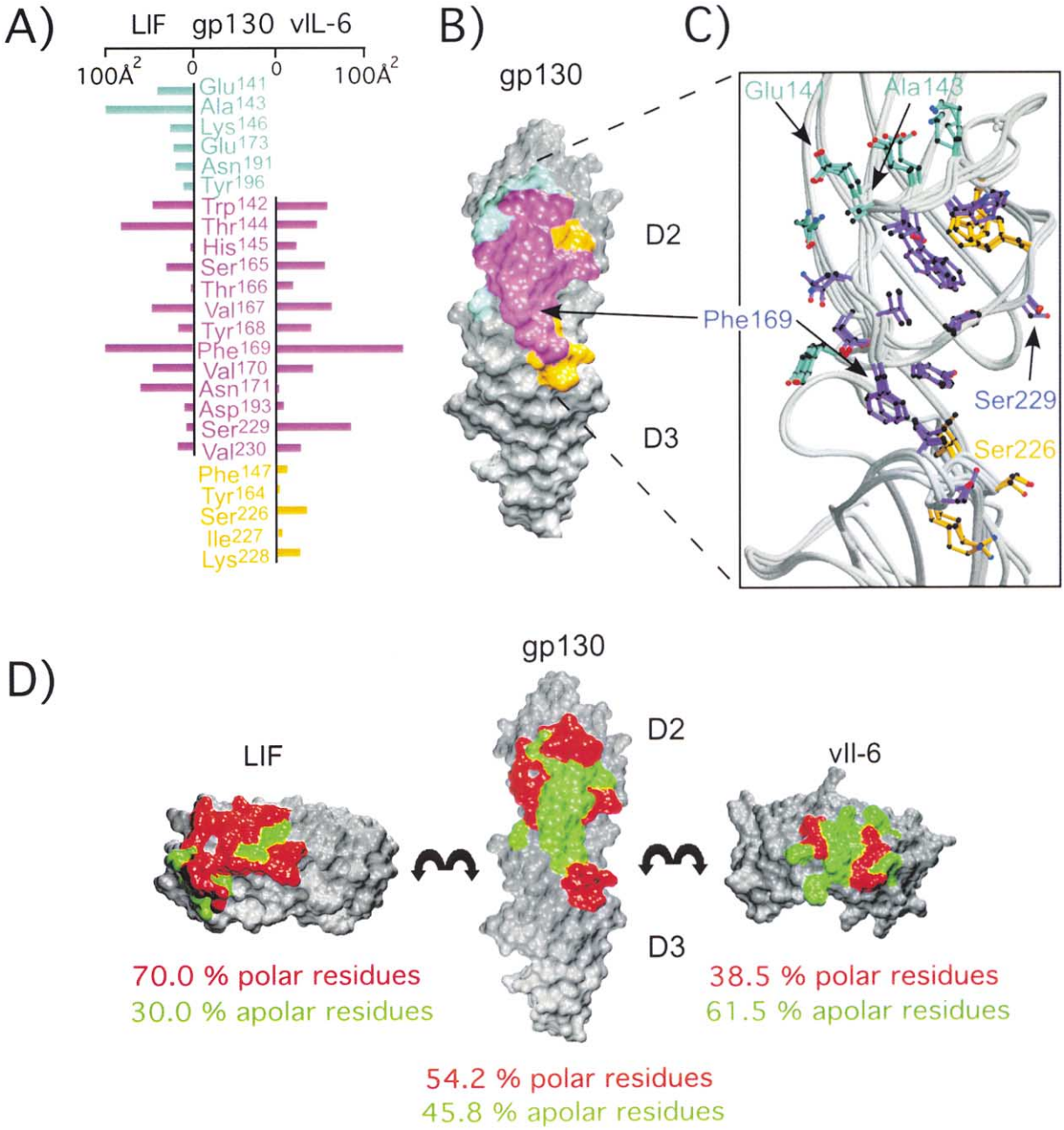

Figure 3. Comparative Analysis of the Buried Surface Residues of gp130-CHR when Bound to LIF or Viral IL-6

Residues contributing to the buried surface area of the interface, as calculated using the Protein-Protein Interaction (PPI) server http://www.biochem.ucl.ac.uk/bsm/PP/server, are (A) graphically displayed on a vertical histogram showing relative buried surface areas in Å^2 and (B) mapped onto the surface of gp130. Residues colored in cyan are exclusive to LIF binding, residues in purple are shared between LIF and viral IL-6 and residues in yellow are exclusive to viral IL-6. (C) A least squares superposition of three gp130 structures showing the rigidity of the buried contact residues on gp130 from unliganded gp130 and the viral IL-6 and LIF complexes. (D) Polarity of the residues forming the contact surfaces of LIF and viral IL-6 and their respective docking sites on gp130CHR. Hydrophobic residues are colored as green surface and hydrophilic residues a red surface. Note the significant hydrophilic contact surface of LIF relative to the primarily hydrophobic contact surface of viral IL-6. VMD (Humphrey et al., 1996) was used to prepare MSMS surface representations (Sanner et al., 1996).

surface contributes more than 60% of the buried surface area (Figure 3D). This hydrophobic interface has sufficiently high affinity with gp130 to alleviate the requirement for an α receptor, as necessitated for human IL-6 to bind gp130 (Boulanger et al., 2003). Seven of the thirteen residues that form the shared gp130 binding surface between LIF and viral IL-6 form a continuous hydrophobic patch, with the conserved and protruding Phe^{169} centrally disposed (Bravo et al., 1998; Horsten et al., 1997; Kurth et al., 2000). Furthermore, Phe^{169} contributes the largest fraction of buried surface area in the LIF-gp130 interface (113 Å^2) the viral IL-6-gp130 interface

Table 2. Comparison of the Dominant Side-Chain Contributions to the Free Energy of Binding for Complexes of gp130 with Viral IL-6 and LIF

gp130 residues		$\Delta\Delta G^{bind}_{LJnet}$		$\Delta\Delta G^{bind}_{Solv}$		$\Delta\Delta G^{bind}_{HBnet}$		$\Delta\Delta G^{bind}_{res}$	
		vIL6	LIF	vIL6	LIF	vIL6	LIF	vIL6	LIF
Glu	141	0.0	1.9	0.0	−1.4	0.0	0.8	0.0	1.3
Trp	142	2.1	1.8	−0.2	−0.2	0.0	0.0	1.9	1.6
Thr	144	0.6	1.0	−0.5	−0.4	0.0	1.0	0.1	1.6
His	145	0.4	0.0	−0.2	0.0	0.0	0.0	0.2	0.0
Lys	146	0.0	0.4	0.0	−0.5	0.0	0.0	0.0	−0.1
Ser	165	0.2	0.2	−0.4	−0.3	0.8	0.6	0.6	0.5
Val	167	1.2	0.9	0.2	0.0	0.0	0.0	1.4	0.9
Tyr	168	0.9	0.1	−0.2	−0.1	0.0	0.0	0.7	0.0
Phe	169	3.2	2.3	−0.5	−0.5	0.0	0.0	2.7	1.8
Val	170	0.9	1.2	−0.4	−0.3	0.0	0.0	0.5	0.9
Asn	171	0.0	1.4	0.0	−1.0	0.0	0.6	0.0	1.0
Glu	173	0.0	0.9	0.0	−0.7	0.0	0.0	0.0	0.2
Asn	191	0.0	0.5	0.0	−0.3	0.0	0.0	0.0	0.2
Asp	193	0.2	0.5	−0.3	−0.5	0.0	1.5	−0.1	1.5
Val	195	0.0	0.0	0.0	0.0	0.0	0.0	0.0	0.0
Ser	226	0.1	0.0	−0.1	0.0	0.0	0.0	0.0	0.0
Ser	229	0.2	0.0	−0.3	0.0	0.0	0.0	−0.1	0.0
Val	230	0.6	0.2	−0.2	−0.1	0.0	0.0	0.4	0.1
	all	10.7	13.4	−3.1	−6.3	0.7	3.9	8.3	11.5

The underlined numbers denote an energetic difference for interaction of a shared gp130 residue with LIF or viral IL-6 of $\geq$ 0.5 kcal/mole. Shown are changes in binding free energy ($\Delta\Delta G^{bind}$) obtained by computational alanine scanning mutagenesis (Kortemme and Baker, 2002). $\Delta\Delta G^{bind}_{LJnet}$: contributions of attractive and repulsive Lennard-Jones interactions, $\Delta\Delta G^{bind}_{Solv}$: contribution of solvation, $\Delta\Delta G^{bind}_{HBnet}$: contributions of sidechain-sidechain and sidechain-backbone hydrogen bonding. $\Delta\Delta G^{bind}_{res}$: total contribution of the side-chain (beyond the Cβ atom) to the binding free energy. Energies are in kcal/mol. The solvation term reflects the loss of interactions with solvent when polar atoms are buried in an interface, and counteracts attractive van-der-Waals and hydrogen bonding interactions made with other protein atoms.

(127 Å^2) (Chow et al., 2001), as well as the human IL-6 hexamer site II (128 Å^2) (Boulanger et al., 2003). We suggest that the shared patch on gp130, anchored by Phe^{169}, forms the primary molecular determinant for complex formation, while the surrounding residues utilize an extreme chemical flexibility, involving both main-chain and side-chain, to form interactions appropriate to the surface chemistry of each of the ten cytokines which bind gp130. We propose "thermodynamic plasticity" that is relatively insensitive to ligand structure, rather than conformational plasticity that is a structural adaptation to ligand, as a means of degenerate ligand recognition by gp130.

Thermodynamic Plasticity as New Mechanism to Enable Crossreactivity

Our hypothesis of thermodynamic plasticity as a means for degenerate ligand recognition is further supported by the results of a computational analysis of the dominant contributions to the binding free energy in gp130-cytokine complexes (Table 2). Computational alanine scanning mutagenesis (Kortemme and Baker, 2002) uses a simple physical model to replace contact residues in a protein-protein interface individually with alanine, and then estimates the change in binding free energy caused by the deletion of side-chain beyond the Cβ atom. A comparison of the contributions of van-der-Waals packing interactions, solvation, and hydrogen bonding of individual side chains in the complexes of gp130 with viral IL-6 and LIF (Table 2) illustrates the different strategies used by the two ligands to bind to largely overlapping interfaces on gp130: while LIF forms mainly polar and solvent interactions to recognize peripheral polar moieties on gp130 (e.g., $\Delta\Delta G^{bind}_{HBnet}$ and $\Delta\Delta G^{bind}_{Solv}$, respectively), viral IL-6 appears to optimize hydrophobic packing interactions in the interface center ($\Delta\Delta G^{bind}_{LJnet}$). Glu^{141}, Asn^{171}, and Glu^{173} make sidechain-sidechain hydrogen bonds in the LIF complex but not the viral IL-6 complex (Table 2, columns 7 and 8), whereas Phe^{169} (Bravo et al., 1998; Horsten et al., 1997; Kurth et al., 2000), Tyr^{168}, Val^{167}, and Val^{230} all show stronger attractive van-der-Waals interactions in the vIL-6 complex (Table 2, columns 3 and 4). Notably, Thr^{144} uses its hydrogen bonding capability in the LIF complex and makes hydrophobic interactions in the viral IL-6 complex. Importantly, the results of this computational Ala-scan are consistent with known experimental and mutational data for gp130, particularly the identification of Phe^{169} as the "hotspot" for cytokine recognition (Bravo et al., 1998; Horsten et al., 1997; Kurth et al., 2000).

More generally, gp130-cytokine recognition can be compared and contrasted with other examples of "consensus" binding sites for small molecules (Mattos and Ringe, 1996; Schumacher et al., 2001), as well as protein interfaces capable of recognizing structurally diverse ligands (DeLano et al., 2000). Two general principles to achieve degeneracy in protein-mediated recognition have been pointed out. (1) Structural plasticity allowing the receptor to adapt to various ligands by conformational change involving side chains as well as the backbone (Atwell et al., 1997; Sundberg and Mariuzza, 2000) or (2) simultaneous presentation to ligands of polar and hydrophobic binding capabilities which are *both* simultaneously satisfied by each of the various ligands (DeLano et al., 2000; Schumacher et al., 2001). The chemical character gp130 cytokine binding site is reminiscent of the second mode of interaction, with structurally fixed

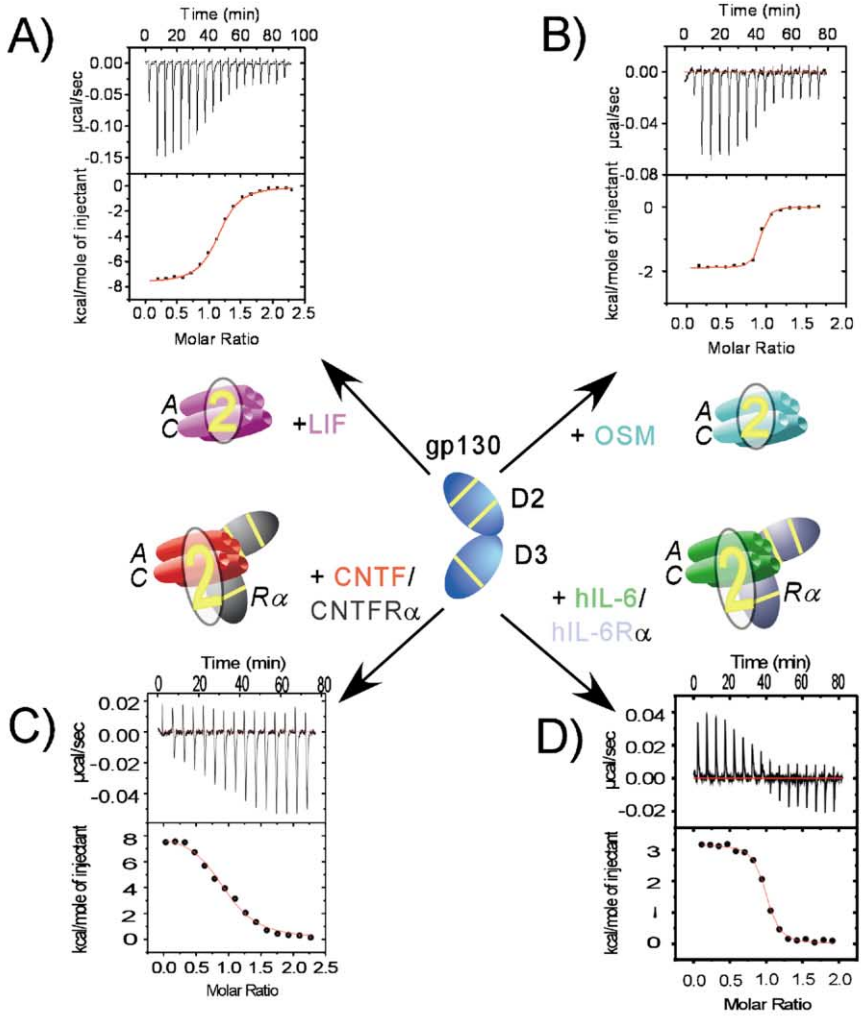

E)

	LIF	OSM	CNTF/ CNTFRα	hIL-6/ hIL-6Rα
Δ H kcal/mol	-7.7 ± 0.07	-1.9 ± 0.02	8.3 ± 0.54	3.3 ± 0.3
Δ S cal/(molK)	5.3	30	62	45
Δ Cp cal/mol/K	-245	-212	-340	-490
Δ G kcal/mol	-9.2	-10.3	-9.0	-9.6
K_D nM	80 ± 6.2	11.8 ± 2.8	103 ± 20	35 ± 5
T(K)	283	283	280	281
n	1.1 ± 0.006	1.0 ± 0.005	0.9 ± 0.037	1.0 ± 0.016

Figure 4. Thermodynamic Basis for gp130 Promiscuity

Isothermal titration calorimetry of the binary complexes of (A) LIF-gp130CHR, (B) oncostatin M (OSM)-gp130CHR, (C) CNTF/CNTFRα-gp130CHR, and (D) hIL-6/hIL-6Rα-gp130CHR. Data points in (A) through (D) are fit with a best-fit curve with non-linear least squares fitting. The measured and calculated thermodynamic parameters for each of the four titrations are presented in tabular format in (E). Each titration shows favorable entropy (ΔS), albeit to varying degrees.

residues forming a cluster of hydrophobic residues in the center surrounded by polar groups in the periphery. However, an important distinction is that the amphipathic binding capabilities of the gp130 site are used in distinctly different ways by different ligands (viral IL-6 and LIF), exploiting predominantly *either* the hydrophobic (viral IL-6) *or* the polar moieties (LIF). Thus, gp130 appears to utilize thermodynamic plasticity as a third, novel principle of protein-mediated recognition.

While structural plasticity has the advantage that quite different ligand surfaces can be recognized, there is a necessary accompanying loss in affinity associated with the fixing of one of the alternative receptor sidechain-backbone conformations. In contrast, less receptor conformational entropy loss need occur in the fixed recognition strategy since the binding residues can have optimal interactions in the unbound state that are unchanged upon binding. Because of the reduced entropy loss associated with the fixed recognition strategy, as is the case with gp130 cytokine recognition, not all individual interactions need be optimized or utilized.

Experimental Thermodynamic Basis of gp130 Promiscuity

To complement the structural and computational analysis of the LIF-gp130 interface, the thermodynamics of ligand-receptor association were experimentally measured using isothermal titration calorimetry (ITC) (Figure 4A). The LIF/gp130 interaction displays a moderate affinity (K_D = 80 nM), with favorable enthalpic contributions, $\Delta H = -7.7$ kcal/mol for LIF + gp130 CHR, consistent with the highly polar interface observed in the LIF-gp130 complex (polar interactions are predominantly exothermic). Surprisingly, in apparent contrast to the bound water network observed in the LIF-gp130 interface (Figure 2B), the entropy is *favorable* ($\Delta S = +5.3$ cal/(molK) for LIF–gp130CHR. Hence, in spite of the unfavorable entropic penalty for trapping waters, there is still overall entropically favorable desolvation (i.e., expulsion of waters) during complex formation. Herein may lie the mechanism of thermodynamic plasticity. The highly exposed, amphipathic binding site of gp130 may contain an extraordinary ability to order water. A broad "dynamic range" in the extent of desolvation may serve as a structurally insensitive mechanism to expand gp130's ability to bind cytokine surfaces of contrasting surface chemistry and structure. The ΔCp of the LIF-gp130 interaction, calculated from the temperature dependence of the enthalpy, is a rather large and negative value of –245 cal/mol/K, which is also characteristic of desolvation within a protein interface.

The concept of a universal thermodynamic solution, for binding structurally diverse cytokine surfaces, is supported by companion ITC measurements between oncostatin-M, ciliary neurotrophic factor and human IL-6, site II with the gp130 CHR (Figures 4B–4D) (note: the gp130 D1 is not involved in the interactions, thus the D1D2D3 and D2D3 gp130 constructs yield similar ITC results, see Figure 1C). In all cases, the interactions are primarily entropy-driven desolvation processes [human IL-6: 45 cal/(molK), OSM: 30 cal/(molK) and CNTF: 62 cal/(molK)], albeit to varying extents commensurate with the surface polarity of the cytokine in the site II. For instance, the highly polar LIF showed the least desolvation and largest enthalpy. The ITC measurements, then, vividly reveal the underlying basis of crossreactivity, which was suggested by structure and computation. Hence, there appears to be divergent structural solutions for gp130 recognition of cytokine, but a convergence in the overall thermodynamic properties underlying the recognition.

For comparative purposes, we attempted ITC measurements with viral IL-6 and gp130, but the extreme hydrophobicity of the viral IL-6 site II surface causes aggregation even at low protein concentrations, and requires detergent for solubility, which is incompatible with the sensitive ITC measurements. Interestingly, viral IL-6 is highly soluble when complexed with gp130, which shields the hydrophobic surface from solvent. We would expect that the viral IL-6/gp130 interaction is more entropically favorable than LIF-gp130 due to expulsion of waters from the apolar interface, and viral IL-6 represents the hydrophobic extreme for a gp130-ligand.

In contrast to the entropically favorable, promiscuous interactions of the shared receptor gp130 with cytokines, we also measured the thermodynamics, using ITC, of the highly specific site I interactions between both IL-6 and CNTF and their respective α-receptors (data not shown). We find that these interactions are highly exothermic and *entropically unfavorable*, consistent with the polar and charged nature of these interfaces, as defined by both structure and mutagenesis (Deller et al., 2000; Kalai et al., 1997). Hence, the gp130-cytokines have evolved one specific, nondegenerate binding epitope (site I) to utilize structurally sensitive interactions such as hydrogen bonds and salt-bridges for recognition by their specific receptors, but an opposing binding interface (site II) recognized by the shared receptor that is energetically much less structurally sensitive and primed for crossreactivity.

LIF/LIF-R/gp130 Assembles through Noncooperative Energetics to Form a Hetero-Trimeric Complex

In the absence of structural information on the complete LIF/gp130/LIF-R complex, stepwise thermodynamic measurements of the individual receptor-cytokine interactions can provide a detailed picture of the composition, and assembly pathway of the higher-order signaling complex. The interaction between LIF and LIF-R is through the LIF site III, which shares the same conserved phenylalanine and lysine as the site III of OSM. (Figure 5) The analogous paradigm was established in the viral and human IL-6 complexes, which use a single conserved tryptophan (Figure 5) to form the site III that interacts with the receptor "Ig domain," which is located at the D3 domain of LIF-R (Figure 1A). A high affinity was measured between LIF and LIF-R ($K_D \sim 1$ nM) similar to what has been measured using cellular assays (Hudson et al., 1996; Moreau et al., 1988). The large favorable entropy (22 cal/(molK) indicates that solvent is excluded from the interface, and is consistent with mutagenesis studies of LIF that has identified a conserved aromatic (Phe) as the energetic "hotspot" of the site III interface of LIF, OSM, and CNTF with LIF-R (Bravo et al., 1998; Horsten et al., 1997; Kurth et al., 2000).

The titration of gp130-D1D2D3 into the preformed hetero-dimeric complex of LIF and LIF-R and the converse of LIF-R into the preformed complex of LIF/gp130-

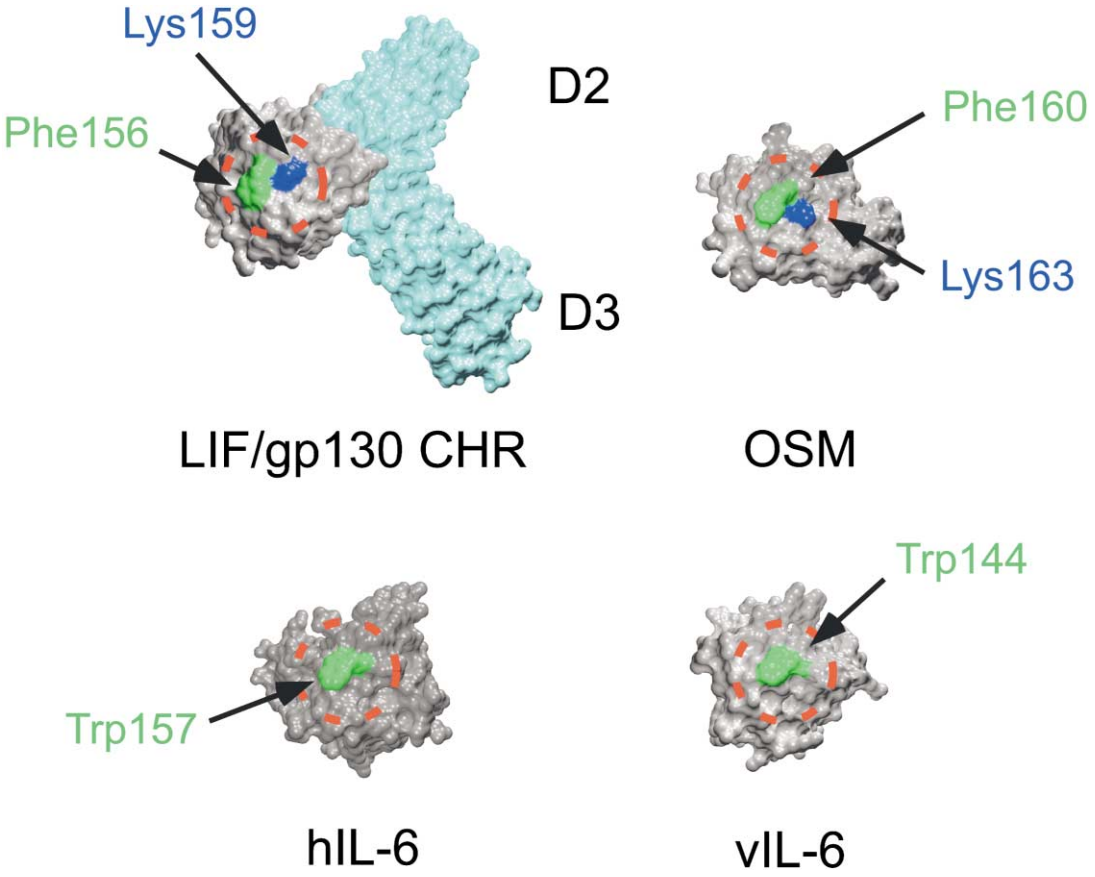

Figure 5. Surface Representations Showing the Site III Interfaces of LIF OSM, IL-6, and Viral IL-6

The site III LIF and OSM, which engage LIF receptor (LIFR) is defined by both a conserved phenylalanine and a lysine residue. The structural paradigm for site III has been established with hIL-6 (Boulanger et al., 2003) and viral IL-6 (Chow et al., 2001), where the hot spot residue is a single tryptophan that engages the Ig domain of gp130.

D1D2D3 displayed similar thermodynamic profiles to the binary titrations of LIF with LIF-R (Figure 6A and 6B). Hence, precomplexation of LIF with either gp130 or LIF-R does not influence binding to the other receptor, indicating assembly of the LIF signaling complex proceeding through non-cooperative energetics. Multi angle light scattering (MALS) of the complexes formed by ITC showed the molecular mass to be 118 kDa consistent with a heterotrimeric assembly including one copy each of LIF, gp130 and LIF-R (Figure 6B). From the structural and thermodynamic data presented here we propose an assembly model where LIF initially binds through its site III to the Ig domain of LIF-R in a single binding event with affinity of approximately 1 nM. Gp130 is then recruited and binds the site II of LIF with an affinity of approximately 80 nM at the elbow of the CHR domain. The heterotrimeric assembly appears to tolerate initial engagement of either site II or III as there is no observed energetic coupling between these sites. As for the gp130-homodimeric cytokines, recent data suggests that the three membrane proximal domains may associate during receptor activation (Timmermann et al., 2002; Voisin et al., 2002).

The question of how the "symmetry" of the hexameric blueprint seen in the IL-6-type cytokines (Boulanger et al., 2003) can be broken to accommodate two *different* shared receptors appears resolved. The non-cooperative assembly mechanism of the LIF-R/gp130 heterodimeric cytokines, such as LIF, CNTF, NNT1-BSF3, contrasts with the cooperative assembly of the gp130 homodimeric cytokines such as IL-6, IL-11 and viral IL-6. The explanation lies in the presence of high affinity site III interactions in the LIFR/gp130 cytokines obviating the requirement for an avidity-enhancing higher-order hexamer formation (Figure 6D). The transition of the homodimeric gp130-cytokines (i.e., IL-6) from the trimolecular to the hexameric structure is necessitated by their inherently weak site III interactions requiring high local concentrations of the site III that is achieved by "doubling" of the complex. Whereas the high affinity site III of LIF (also OSM and CNTF-data not shown) is sufficient to stabilize the heterotrimer without the need for a transition to a high-order assembly. The blueprint established for the gp130 homodimer in the IL-6 hexamer (Boulanger et al., 2003), is utilized by the gp130-LIFR cytokines, except that one gp130 molecule is replaced by LIF-R at the site III interaction, resulting in a reduced stoichiometry (Figure 6C).

Thermodynamic and Interaction Plasticity as New Mechanisms Enabling Crossreactivity

To summarize, our results reveal two components of plasticity:

(1) As the receptor has very similar conformation in

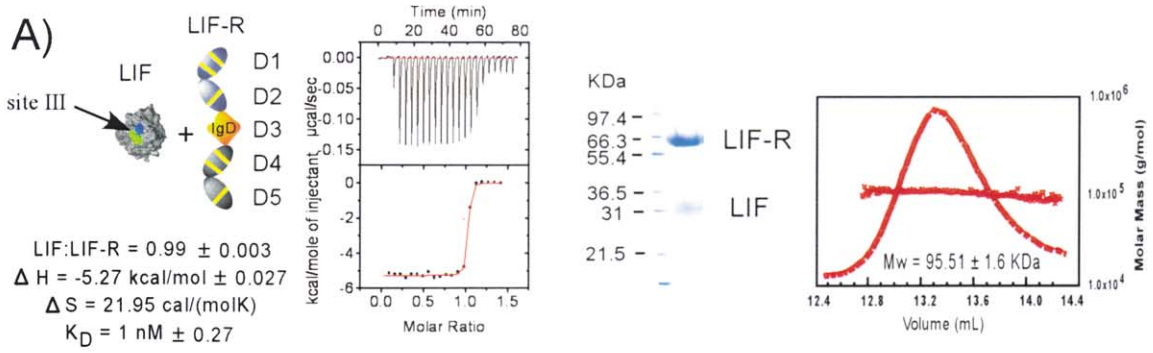
A)
LIF-R
LIF
site III
D1
D2
D3
D4
D5
IgD
LIF:LIF-R = 0.99 ± 0.003
Δ H = -5.27 kcal/mol ± 0.027
Δ S = 21.95 cal/(molK)
K_D = 1 nM ± 0.27
Time (min)
0 20 40 60 80
0.00
-0.05
-0.10
-0.15
µcal/sec
0
-2
-4
-6
kcal/mole of injectant
0.0 0.5 1.0 1.5
Molar Ratio
KDa
97.4
66.3
55.4
36.5
31
21.5
LIF-R
LIF
Mw = 95.51 ± 1.6 KDa
12.4 12.8 13.2 13.6 14.0 14.4
Volume (mL)
1.0x10^6
1.0x10^5
1.0x10^4
Molar Mass (g/mol)

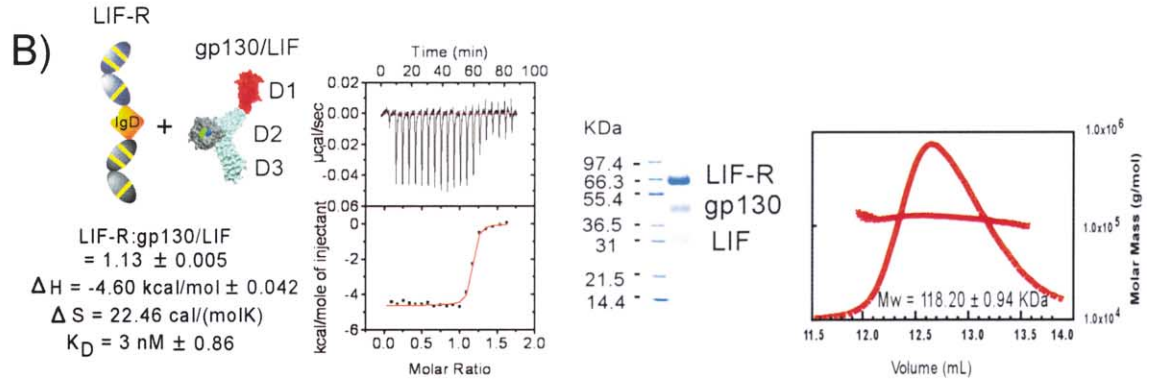
B)
LIF-R
gp130/LIF
D1
D2
D3
IgD
LIF-R:gp130/LIF
= 1.13 ± 0.005
Δ H = -4.60 kcal/mol ± 0.042
Δ S = 22.46 cal/(molK)
K_D = 3 nM ± 0.86
Time (min)
0 20 40 60 80 100
0.02
0.00
-0.02
-0.04
-0.06
µcal/sec
0
-2
-4
-6
kcal/mole of injectant
0.0 0.5 1.0 1.5 2.0
Molar Ratio
KDa
97.4
66.3
55.4
36.5
31
21.5
14.4
LIF-R
gp130
LIF
Mw = 118.20 ± 0.94 KDa
11.5 12.0 12.5 13.0 13.5 14.0
Volume (mL)
1.0x10^6
1.0x10^5
1.0x10^4
Molar Mass (g/mol)

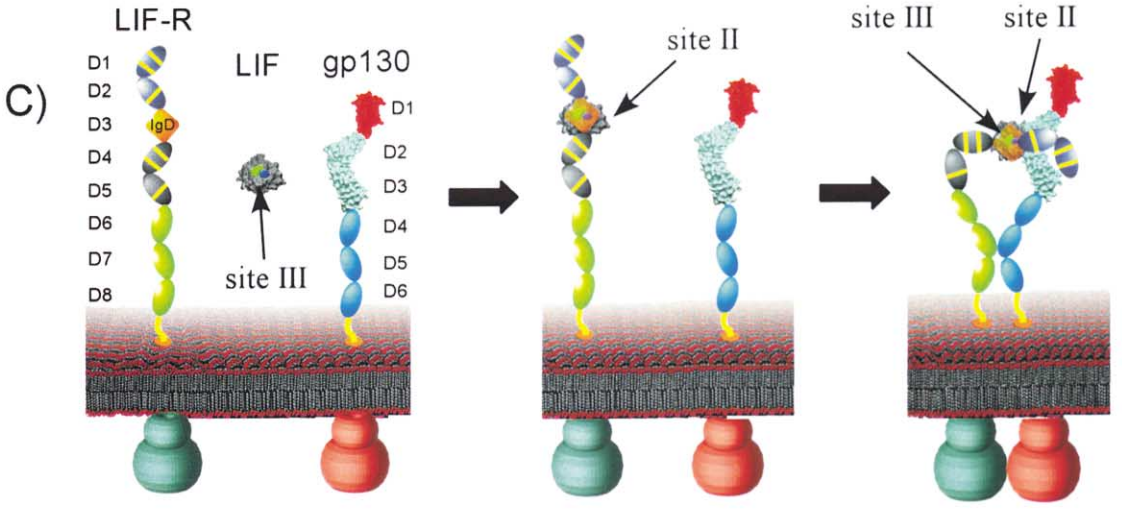
C)
LIF-R
D1
D2
D3
D4
D5
D6
D7
D8
IgD
LIF
site III
gp130
D1
D2
D3
D4
D5
D6
site II
site III
site II

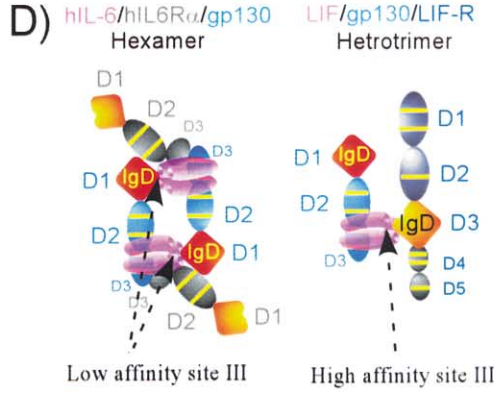
D)
hIL-6/hIL6Rα/gp130
Hexamer
LIF/gp130/LIF-R
Hetrotrimer
D1
D2
D3
IgD
Low affinity site III
High affinity site III

the different complexes, it has evolved a way of using an identical surface to recognize chemically different ligands. It does this by using only part of this surface as a binding energy hot spot in the different complexes. This energetically important part is different in the two complexes, as it appears to "match" the different chemical nature of the ligand surface by selecting either the polar or the hydrophobic interaction capabilities. This is substantially different from two other mechanisms of how a receptor can recognize different ligands that have been described previously: (a) the receptor adapts structurally (induced fit) or (b) all binding capabilities are used but in different ways (Delano et al., 2000).

(2) The second component is the thermodynamic *basis* of the plasticity. How can a receptor still achieve reasonable binding affinity if only a part of the interaction capabilities of the interface are used in each complex? A possible thermodynamic mechanism of this plasticity is suggested by the observation that all four complexes studied by calorimetry display a favorable entropy upon binding while the enthalpy is not favorable in some cases. gp130 appears to use a large entropy "storage" to compensate for a range of enthalpies observed in the different complexes, that can be unfavorable when interacting with a very hydrophobic partner like vIL-6 that does not satisfy the polar interaction capabilities on the receptor surface. The likely mechanism for the favorable gain in entropy is the release of bound waters that drives complex formation in all cases, although to varying extents (decreasing with increasing polarity of the ligand interface).

In order to achieve this energetic plasticity, the surface of gp130 has evolved special properties to act as a degenerate receptor. The binding site is rich in amino acids capable of participating in both polar and nonpolar interactions, such as Arginine, Tyrosine, and Tryptophan. We clearly see in the different gp130 complex structures that each of these amino acids is optimized such that its apolar features are primarily used for interaction with the cytokine, while projecting the polar ends out of the interface into solvent.

Numerous shared receptors exist, such as the common γ chain (γc) for IL-2, IL-4, IL-7, IL-13, IL-15, and others. The common β chain for IL-5, etc. But there are also strikingly cross-reactive receptors in the nervous system such as the p75 Nerve Growth Factor receptor and the recently described Nogo receptor (Chen et al., 2000; GrandPre et al., 2000; Prinjha et al., 2000). Further biophysical studies are required to determine the cross-reactive nature of these receptors.

Experimental Procedures

General Protein Expression and Purification

All proteins used in this study were expressed using the Baculovirus system (Pharmingen) in insect cells. The D2D3 CHR domain of gp130, including residues 101 to 302, and full length LIF (residues 1 to 180) were cloned into the pAcgp67A vector (Pharmingen). The primers (available upon request) were designed to be in frame with the gp67A signal sequence of the vector and included a C-terminal hexa-histidine tag. After infection of cell with recombinant virus, the supernatant was harvested through a two-step centrifugation process to remove cellular material, and reduced in volume using tangential flow concentration. Ni-NTA resin were added to the concentrated supernatant and allowed to "batch" bind at 4°C, and elution fractions from the Ni-NTA resin containing the protein of interest as determined by SDS-PAGE analysis were concentrated using Centricon (Millipore, Bedford, MA) spin concentrators and injected onto an FPLC gf200 sizing column.

Additional Steps for Crystallization Quality Protein

The extensive N-linked glycosylation observed with both gp130 D2D3 and LIF resulted in heterogeneous proteins with many glycoforms apparent on an SDS-PAGE gel. To eliminate the N-linked glycans of these molecules, both were expressed in the presence of tunicamycin (0.3 – 0.5 μg/ml), a potent inhibitor of N-linked glycosylation. The use of tunicamycin decreased the overall protein yields but did not affect binding between LIF and gp130 as determined by both calorimetry (our work) and surface plasmon resonance (Bravo et al., 1998) and the glycosylations have also been shown to be dispensable in biological activity assays (Robinson et al., 1994). The hexa-histidine tag was also removed from proteins to be used in crystallization with an overnight digest of carboxypeptidase A (1:100) 4°C prior to injection onto the FPLC.

Crystallization, Data Collection, and Processing

Purified LIF and gp130 D2-D3 were mixed in stoichiometric amounts to produce the binary complex with a final concentration of 7mg/ml. Injection of a small sample of the complex onto the FPLC sizing column showed one peak that eluted with the expected size of the binary complex. Small plate-like crystals measuring less than 0.05 Å in the longest dimension were initially obtained in 0.5 μl sitting drops with equal volumes of LIFD2 complex (7 mg/ml) and mother liquor (8%–10% polyethylene glycol 3350, 0.2 M sodium iodide, 0.1 M imidazole pH 7.5). These conditions produced crystals that grew in space group $P2_12_12_1$ with two binary complexes in the asymmetric unit of the orthorhombic cell (a = 79.91, b = 87.05, c = 147.63). With two molecules in the assym. unit, the Mathews coefficient was calculated to be 2.8 Å^3/Da with approximately 50% solvent content. X-ray diffraction to 2.5 Å was collected at the Lawrence Berkeley National Laboratory on beamline 8.2.1 using a 2×2 CCD detector to collect 90 s images. To obtain quality diffraction images that could be processed, the crystals required annealing where the cryo stream was blocked for 1 s resulting in sharp diffraction spots. The data were integrated and scaled with DENZO and SCALEPACK (Otwinowski and Minor, 1997). Data collection and refinement statistics are presented in Table 1.

Structure Solution and Refinement

Initial phases were obtained by molecular replacement with MOLREP (Vagin and Teplyakov, 1997) using the coordinates of murine

Figure 6. Higher Order Assembly of LIF, gp130D1D2D3, and LIF-R as Measured by Isothermal Titration Calorimetry

(A) LIF titrated into LIF-R (B) LIF-R titrated into the LIF-gp130D1D2D3 binary complex (note: the presence or absence of the gp130 D1 domain has no effect on the measurements, data not shown). The higher order complexes from the ITC cell were purified on the FPLC, visualized on an SDS-PAGE gel and the molecular mass characterized by multi-angle light scattering (MALS). The binary titration of LIF into LIF-R shows the same K_D as LIF-R into the pre-formed complex of LIF-gp130 indicating that the hetero-trimeric complex assembles through non-cooperative energetics. (C) Assembly model of the hetero-trimeric LIF/gp130/LIF-R complex. Initiation of assembly proceeds with LIF binding through its site III interface to the Ig domain of LIF-R. Gp130 is then recruited to this heterodimeric complex and binds to the site II of LIF. We have shown here that assembly proceeds through non-cooperative energetics indicating that there is no favorable contact between gp130 and LIF-R, and that the final assembly is a heterotrimer with one copy each of LIF, gp130 and LIF-R. (D) Orthogonal top view of the hIL-6 hexamer (Boulanger et al., 2003) and the LIF/gp130/LIF-R heterotrimer illustrating the structural role for the weak affinity site III of hIL-6 that binds to the D1 domain of gp130 and the high affinity site III of LIF that binds to the LIF-R.

LIF structure PDB – 1LKI (Robinson et al., 1994) and the D2D3 domains of gp130 from the viral IL-6 – tetramer PDB – 1I1R (Chow et al., 2001) as search models. The data was refined to a final resolution of 2.5 Å with CNS (Brunger et al., 1998) using density modification (DM), which included solvent flipping and strict 2-fold noncrystallographic symmetry (NCS) averaging where LIF, gp130D2 and gp130D3 did not exceed a root mean squared deviation (r.m.s.d.) of 0.06 Å from their respective NCS partners. The model was visualized and built into the electron density map using the program O (Jones et al., 1991). Several rounds of refinement resulted in an overall R_{cryst} of 24.8% and an R_{free} of 28.7%. The final model of LIF begins at residue Cys^{12} and ends at Phe^{180} while the gp130 model incorporates residues Gly^{101} to Glu^{301}. Stereochemical analysis of the refined LIF – gp130 D2-D3 structure was performed with PROCHECK (Laskowksi et al., 1993) with the Ramachandran plot showing good stereochemistry with 86.5% of the residues in the favored conformations and no non-glycine residues modeled in disallowed orientations. Clear electron density permitted modeling of all but the first eight N-terminal main chain atoms of LIF. Within the framework of the modeled main-chain, three side-chains of gp130 residues (Ser^{211}, Glu^{212} and Glu^{213}) were changed to Gly and five side-chains on the surface loop incorporating residues 149 to 154 of LIF (Asp^{149}, Thr^{150}, Ser^{151}, Lys^{153} and Asp^{154}) were changed to Gly. Solvent molecules were added using the program WATERPICK (Brunger et al., 1998). Overall, the asymmetric unit contains 736 residues, 2 iodide ions that bind at crystal contacts and 192 solvent molecules.

Isothermal Titration Calorimetry

Calorimetric titrations were carried out on a VP-ITC calorimeter (MicroCal, Northhampton, MA) at 6,10,15 and 20°C for each of the binary complexes and at 10°C for the higher order assembly of the heterotrimer. Prior to each titration, the protein samples were degassed for 10 min. Data was processed with the MicroCal Origin 5.0 software. The same buffer of 10 mM HEPES (pH 7.5) supplemented with 200 mM sodium chloride was used in each experiment to control for buffer heat dilution effects. In the titrations of the binary complexes, either gp130 D2D3, gp130 D1D3 or LIF-R was used in the cell at a concentration of 3–5 μM and LIF in the syringe at a concentration of 40–50 μM. In the titrations of the higher order heterotrimer, LIF in the cell was saturated in the first series of experiments with LIF-R followed by gp130 D1D3 and the reverse order of the receptors in the second series of experiments. As a final control, the contents of the cell following each titration was injected onto the gf200-sizing column on the FPLC to ensure the proteins had not aggregated during the experiment and finally visualized on an SDS-PAGE gel to ensure the presence of all proteins of the complexes.

Multiangle Light Scattering

A DAWN EOS (Wyatt Technology, Santa Barbara, CA) equipped with a K5 flow cell and a 30 mW linearly polarized GaAs laser of wavelength 690 nm was used in all experiments. All measurements were made in the in-line flow mode. A Jasco Model PU-980 (Jasco Corp, Tokyo, Japan) pump was used to flow 0.1 μm filtered solvent (10 mM HEPES [pH 7.5] and 200 mM NaCl) through a Shimadzu DGU-14A (Shimadzu Corp., Kyoto, Japan) degasser and into an HR 10/30 Superdex-200 (Amersham Biosciences, Piscataway, NJ) gel filtration column. The sample was at approximately 2 mg/ml (in the eluent buffer). Both the light scattering unit and the refractometer were calibrated as per the manufacturer's instructions. A value of 0.185 ml/g was assumed for the dn/dc of the protein. Light scattering data was used from 11 detectors ranging from 50.0° to 134.0° (detectors 6 through 16). The detector responses were normalized by measuring the signal from monomeric bovine serum albumin. The temperature of the light scattering unit was maintained at 25°C and the temperature of the refractometer was maintained at 35°C. The column and all external connections were at ambient temperature (20-22°C). The flow rate was maintained at 0.5 ml/minute throughout the experiments.

Acknowledgments

The authors gratefully acknowledge assistance and helpful discussions with Gerry McDermott, Monika Martick, Fernando Bazan, Stefan Rose-John, John Heath, and Yvonne Jones. The authors would also like to thank Byron DeLaBarre for assistance with the MALS data collection. The authors also acknowledge Stanford Synchrotron Radiation Laboratory and Advanced Light Source for x-ray resources. The authors were supported by the NIH (AI51321), Keck Foundation, CRI, and Pew. M.J.B. is supported by a National Sciences and Engineering Research Council of Canada post-doctoral fellowship.

Received: April 29, 2003
Revised: July 2, 2003
Accepted: July 8, 2003
Published: September 25, 2003

References

Atwell, S., Ultsch, M., De Vos, A.M., and Wells, J.A. (1997). Structural plasticity in a remodeled protein-protein interface. Science *278*, 1125–1128. Bazan, J.F. (1990). Haemopoietic receptors and helical cytokines. Immunol. Today *11*, 350–354.

Benigni, F., Fantuzzi, G., Sacco, S., Sironi, M., Pozzi, P., Dinarello, C.A., Sipe, J.D., Poli, V., Cappelletti, M., Paonessa, G., et al. (1996). Six different cytokines that share GP130 as a receptor subunit, induce serum amyloid A and potentiate the induction of interleukin-6 and the activation of the hypothalamus-pituitary-adrenal axis by interleukin-1. Blood *87*, 1851–1854.

Boulanger, M.J., Chow, D.C., Brevnova, E.E., and Garcia, K. (2003). Hexameric structure and assembly of the interleukin-6/IL-6 alpha-receptor/gp130 complex. Science *300*, 2101–2104.

Bravo, J., Staunton, D., Heath, J.K., and Jones, E.Y. (1998). Crystal structure of a cytokine-binding region of gp130. EMBO J. *17*, 1665–1674.

Brunger, A.T., Adams, P.D., Clore, G.M., Delano, W.L., Gros, P.R.W., Jiang, J.S., Kuszewski, J., Nilges, N., Pannu, N.S., Rice, L.M., and Simonson, T. (1998). Crystallography and NMR system (CNS): a new software system for macromolecular structure determination. Acta. Cryst. *D54*, 905 - 921.

Chen, M.S., Huber, A.B., van der Haar, M.E., Frank, M., Schnell, L., Spillmann, A.A., Christ, F., and Schwab, M.E. (2000). Nogo-A is a myelin-associated neurite outgrowth inhibitor and an antigen for monoclonal antibody IN-1. Nature *403*, 434–439.

Chow, D., He, X., Snow, A.L., Rose-John, S., and Garcia, K.C. (2001). Structure of an extracellular gp130 cytokine receptor signaling complex. Science *291*, 2150–2155.

DeLano, W.L., Ultsch, M.H., de Vos, A.M., and Wells, J.A. (2000). Convergent solutions to binding at a protein-protein interface. Science *287*, 1279–1283.

Deller, M.C., Hudson, K.R., Ikemizu, S., Bravo, J., Jones, E.Y., and Heath, J.K. (2000). Crystal structure and functional dissection of the cytostatic cytokine oncostatin M. Struct. Fold. Des. *8*, 863–874.

Esnouf, R.M. (1997). An extensively modified version of MolScript that includes greatly enhanced coloring capabilities. J. Mol. Graph. *15*, 132–134.

Garcia, K.C., Degano, M., Pease, L.R., Huang, M., Peterson, P.A., Teyton, L., and Wilson, I.A. (1998). Structural basis of plasticity in T cell receptor recognition of a self peptide-MHC antigen. Science *279*, 1166–1172.

GrandPre, T., Nakamura, F., Vartanian, T., and Strittmatter, S.M. (2000). Identification of the Nogo inhibitor of axon regeneration as a Reticulon protein. Nature *403*, 439–444.

Gyotoku, E., Morita, E., Kameyoshi, Y., Hiragun, T., Yamamoto, S., and Hide, M. (2001). The IL-6 family cytokines, interleukin-6, interleukin-11, oncostatin M, and leukemia inhibitory factor, enhance mast cell growth through fibroblast-dependent pathway in mice. Arch. Dermatol. Res. *293*, 508–514.

Hammacher, A., Richardson, R.T., Layton, J.E., Smith, D.K., Angus, L.J., Hilton, D.J., Nicola, N.A., Wijdenes, J., and Simpson, R.J. (1998). The immunoglobulin-like module of gp130 is required for signaling by interleukin-6, but not by leukemia inhibitory factor. J. Biol. Chem. *273*, 22701–22707.

Heinrich, P.C., Behrmann, I., Muller-Newen, G., Schaper, F., and Graeve, L. (1998). Interleukin-6-type cytokine signalling through the gp130/Jak/STAT pathway. Biochem. J. *334*, 297–314.

Hibi, M., Murakami, M., Saito, M., Hirano, T., Taga, T., and Kishimoto, T. (1990). Molecular cloning and expression of an IL-6 signal transducer, gp130. Cell *63*, 1149–1157.

Hilton, D.J., Nicola, N.A., and Metcalf, D. (1988). Purification of a murine leukemia inhibitory factor from Krebs ascites cells. Anal. Biochem. *173*, 359–367.

Hirano, T., Nakajima, K., and Hibi, M. (1997). Signaling mechanisms through gp130: a model of the cytokine system. Cytokine Growth Factor Rev. *8*, 241–252.

Horsten, U., Muller-Newen, G., Gerhartz, C., Wollmer, A., Wijdenes, J., Heinrich, P.C., and Grotzinger, J. (1997). Molecular modeling-guided mutagenesis of the extracellular part of gp130 leads to the identification of contact sites in the interleukin-6 (IL-6).IL-6 receptor.gp130 complex. J. Biol. Chem. *272*, 23748–23757.

Hudson, K.R., Vernallis, A.B., and Heath, J.K. (1996). Characterization of the receptor binding sites of human leukemia inhibitory factor and creation of antagonists. J. Biol. Chem. *271*, 11971–11978.

Humphrey, W., Dalke, A., and Schulten, K. (1996). J. Mol. Graph. *14*, 33.

Jones, T.A., Zhou, J.Y., Cowan, S.W., and Kjeldgaard, M. (1991). Improved methods for building models in electron density maps and the location of error in these models. Acta Crystallogr. *A47*, 110–119.

Kalai, M., Montero-Julian, F.A., Grotzinger, J., Fontaine, V., Vandenbussche, P., Deschuyteneer, R., Wollmer, A., Brailly, H., and Content, J. (1997). Analysis of the human interleukin-6/human interleukin-6 receptor binding interface at the amino acid level: proposed mechanism of interaction. Blood *89*, 1319–1333.

Kortemme, T., and Baker, D. (2002). A simple physical model for binding energy hot spots in protein-protein complexes. Proc. Natl. Acad. Sci. USA *99*, 14116–14121.

Kraulis, P. (1991). MOLSCRIPT: a program to produce both detailed and schematic plots of protein structures. J. Appl. Crystallogr. *24*, 946–950.

Kurth, I., Horsten, U., Pflanz, S., Timmermann, A., Kuster, A., Dahmen, H., Tacken, I., Heinrich, P.C., and Muller-Newen, G. (2000). Importance of the membrane-proximal extracellular domains for activation of the signal transducer glycoprotein 130. J. Immunol. *164*, 273–282.

Laskowksi, R.A., MacArthur, M.W., Moss, D.S., and Thornton, J.M. (1993). PROCHECK: a program to check the stereochecmial quality of protein structures. J. Appl. Crystallogr. *26*, 283–291.

Livnah, O., Stura, E.A., Johnson, D.L., Middleton, S.A., Mulcahy, L.S., Wrighton, N.C., Dower, W.J., Jolliffe, L.K., and Wilson, I.A. (1996). Functional mimicry of a protein hormone by a peptide agonist: the EPO receptor complex at 2.8 A. Science *273*, 464–471.

Mattos, C., and Ringe, D. (1996). Locating and characterizing binding sites on proteins. Nat. Biotechnol. *14*, 595–599.

Merritt, E.A., and Murphy, E.P.M. (1994). Raster3D Version 2.0. A program for photorealistic molecular graphics. Acta Crystallogr. D Biol. Crystallogr. *50*, 869–873.

Moreau, J.F., Donaldson, D.D., Bennett, F., Witek-Giannotti, J., Clark, S.C., and Wong, G.G. (1988). Leukaemia inhibitory factor is identical to the myeloid growth factor human interleukin for DA cells. Nature *336*, 690–692.

Murphy, M., Reid, K., Hilton, D.J., and Bartlett, P.F. (1991). Generation of sensory neurons is stimulated by leukemia inhibitory factor. Proc. Natl. Acad. Sci. USA *88*, 3498–3501.

Otwinowski, Z., and Minor, W. (1997). Processing of X-ray diffraction data collected in oscillation mode. Methods Enzymol. *276*, 307–326.

Patterson, B.K., McCallister, S., Schutz, M., Siegel, J.N., Shults, K., Flener, Z., and Landay, A. (2001). Persistence of intracellular HIV-1 mRNA correlates with HIV-1-specific immune responses in infected subjects on stable HAART. AIDS *15*, 1635–1641.

Prinjha, R., Moore, S.E., Vinson, M., Blake, S., Morrow, R., Christie, G., Michalovich, D., Simmons, D.L., and Walsh, F.S. (2000). Inhibitor of neurite outgrowth in humans. Nature *403*, 383–384.

Robinson, R.C., Grey, L.M., Staunton, D., Vankelecom, H., Vernallis, A.B., Moreau, J.F., Stuart, D.I., Heath, J.K., and Jones, E.Y. (1994). The crystal structure and biological function of leukemia inhibitory factor: implications for receptor binding. Cell *77*, 1101–1116.

Sanner, M.F., Spehner, J.-C., and Olson, A.J. (1996). Biopolymers *38*, 305.

Schumacher, M.A., Miller, M.C., Grkovic, S., Brown, M.H., Skurray, R.A., and Brennan, R.G. (2001). Structural mechanisms of QacR induction and multidrug recognition. Science *294*, 2158–2163.

Simpson, R.J., Hammacher, A., Smith, D.K., Matthews, J.M., and Ward, L.D. (1997). Interleukin-6: structure-function relationships. Protein Sci. *6*, 929–955.

Sundberg, E.J., and Mariuzza, R.A. (2000). Luxury accommodations: the expanding role of structural plasticity in protein-protein interactions. Struct. Fold. Des. *8*, R137–R142.

Taga, T., and Kishimoto, T. (1997). Gp130 and the interleukin-6 family of cytokines. Annu. Rev. Immunol. *15*, 797–819.

Timmermann, A., Kuster, A., Kurth, I., Heinrich, P.C., and Muller-Newen, G. (2002). A functional role of the membrane-proximal extracellular domains of the signal transducer gp130 in heterodimerization with the leukemia inhibitory factor receptor. Eur. J. Biochem. *269*, 2716–2726.

Vagin, V., and Teplyakov, A. (1997). J. Appl. Cryst. *30*, 1022.

Voisin, M.B., Bitard, J., Daburon, S., Moreau, J.F., and Taupin, J.L. (2002). Separate functions for the two modules of the membrane-proximal cytokine binding domain of glycoprotein *190*, the leukemia inhibitory factor low affinity receptor, in ligand binding and receptor activation. J. Biol. Chem. *277*, 13682–13692.

Yamamori, T., Fukada, K., Aebersold, R., Korsching, S., Fann, M.J., and Patterson, P.H. (1989). The cholinergic neuronal differentiation factor from heart cells is identical to leukemia inhibitory factor. Science *246*, 1412–1416.

Accession Numbers

The coordinates for the LIF/gp130 CHR crystal structure have been deposited in the Protein Data Bank with accession code 1PVH.